Tribo-corrosion Performance of Plasma Sprayed Al_2O_3 on Aluminum Alloy for Thermal Barrier Coatings

Essam R.I. Mahmoud,

Department of Mechanical Engineering, Faculty of Engineering, Islamic University of Madinah, Saudi Arabia

emahoud@iu.edu.sa

And

Ali Algahtani,

Department of Mechanical Engineering, Faculty of Engineering, King Khalid University, Saudi Arabia

Research Center for Advanced Materials Science (RCAMS), King Khalid University, Saudi Arabia

alialgahtani@kku.edu.sa

Abstract: Aluminium alloys have attractions to be used for a wide range of applications due to its lower density and the formation of passive film which provide corrosion protection. At high temperature (more than 250 ^{0}C), the passive film may be destroyed, thermally corroded and it will easily be failed by thermal fatigue failures. This work has investigated the enhancements of plasma sprayed Al_2O_3 coating on the performance of 6082-T6 aluminium alloy surface against erosion and corrosion test environments. The study investigates the macro/microstructure and the formed phases of the plasma sprayed Al_2O_3 formed layer. The erosion resistance of the coated layer, in particular, the effect of sand concentration and temperature variations to the aqueous slurry impingement against material properties such as adhesion, ductility, and roughness were investigated. In addition, a series of electrochemistry tests have been conducted to verify the corrosion performance. As a reference, the un-coated 6082-T6 aluminium substrate was instigated in all the experiments. The resulted showed that plasma sprayed Al_2O_3 coating layer had lamellar structure of approximately 86% γ-Al_2O_3 and 14% α-Al_2O_3 phases and contained many voids and porosity. The coated layer shows good corrosion resistance at ambient temperature. At 80 ºC, small amount of ions penetrations was recorded. The coated layer was completely removed after polarizing the solution up to 400 mV for 24 hours. Although there was no stability of the current in the coating during the polarization test, the coating shows lower corrosion current density under static anodic polarization tests compared to the aluminium substrate indicates better corrosion

resistance. It has been shown that the erosion of the coated layer shows linear erosion rate. The erosion rates observed for the coating in elevated temperature are much lower than aluminium substrate. As a result, the erosion resistance of aluminium alloy can be highly improved by plasma sprayed Al_2O_3 coating, especially at high temperature.

Keywords: 6082 Aluminium Alloy; plasma sprayed coating; erosion resistance; Microstructure; Wear resistance; polarization test.

دراسة أداء سبائك الألومنيوم المطلية بحبيبات الألومينا الصلبة عن طريق البلازما في درجات الحرارة العالية

الملخص: تعتبر سبائك الألومنيوم من المواد الصناعية الهامة وذلك لاستخدامها في مجموعة واسعة من التطبيقات بسبب كثافتها المنخفضة وتشكل طبقة طبيعية رقيقة على سطحها توفر لها الحماية من التآكل الكيميائي. في درجات الحرارة العالية أكثر من 250 درجة مئوية، سيتم تدمير هذه الطبقة، وتتآكل حرارياً خاصة عندما تتعرض لعوامل الفشل الحراري في هذه الظروف الصعبة. في هذا العمل ترسيب حبيبات الألومينا **Al2O3** وذلك عن طريق الرش بالبلازما على سطح إحدى سبائك الألومنيوم المهمة واختبار كفاءتها عن طريق اختبار التآكل والبري الميكانيكي. تمت دراسة البنية المجهرية لمعدن الأساس وكذلك البنية المجهرية للطبقة المشكَّلة بالبلازما. تم فحص مقاومة التآكل للطبقة المترسبة، وكذلك تأثير تركيز الرمال وتغيرات درجات الحرارة على خصائص المواد المختلفة، تم إجراء سلسلة من اختبارات التآكل الكيميائي عن طريق سلسلة من الاختبارات للتحقق من أداء المواد المصنعة عند درجات حرارة مختلفة. أظهرت النتائج أن طبقة الطلاء **Al2O3** التي تم رشها بالبلازما كانت لها بنية صفائحية تقارب 86٪ **γ–Al2O3** و14٪ **α–Al2O3** وتحتوي على العديد من الفراغات والمسامية. تُظهر الطبقة المطلية مقاومة جيدة للتآكل في درجة الحرارة العالية. عند 80 درجة مئوية، تم تسجيل كمية صغيرة من اختراقات الأيونات. تمت إزالة الطبقة المطلية بالكامل بعد استقطاب المحلول حتى 400 ملي فولت لمدة 24 ساعة. على الرغم من عدم وجود استقرار للتيار الموجود في الطلاء أثناء اختبار الاستقطاب، إلا أن الطلاء يظهر انخفاض كثافة تيار التآكل في ظل اختبارات الاستقطاب الأنودي الثابت مقارنة مع الركيزة المصنوعة من الألومنيوم، مما يشير إلى مقاومة أفضل للتآكل. لقد ثبت أن تآكل الطبقة المطلية يظهر معدل تآكل خطي. معدلات التآكل التي لوحظت للطلاء في درجة حرارة مرتفعة أقل بكثير من معدن الأساس غير المطلي. نتيجة لذلك، يمكن تحسين مقاومة التآكل لسبائك الألمونيوم بشكل كبير من خلال طلاء **Al2O3** الرش بالبلازما، خاصة في درجات الحرارة العالية.

1. Introduction

Aluminium is a metallic element which has a natural corrosion resistance at room temperature due to the formation of very thin oxide layer (few nanometre thick) on its surface [1]. This dense layer is formed quickly when it is exposed to the environment. The thickness of the layer is dependent

on the environment parameters. Some of the aluminium alloys also possess attractive properties such as strength to weight ratio, low-cost material and good weldability which make them good candidate for wide range of applications such as aerospace, automotive structures, renewable energy, extraction systems, internal combustion engines and gas turbines sectors. The operation temperature of some of these applications is relatively high. When the surface of the aluminium alloys exposed to high temperature for long time, it will easily be oxidized and wearied. Also, relatively amount of heat losses is expected due to their high thermal conductivity [2-4].

Under aggressive environments, aluminium is subjected to different types of severe corrosion like intergranular corrosion, pitting corrosion, and many other cracks such as stress corrosion cracking [5-6]. Pitting corrosion usually attacks aluminium surfaces causing localised holes in the protective film under chloride corrosive environments which affect the mechanical properties of the metal like reducing the tensile stress and causing fatigue and stress corrosion cracks [7]. For some applications, the materials are suffered from many severe conditions of erosion/wear and corrosion. It led to an irreversible materials degradation, and whenever they take place simultaneously, the process is known as tribo-corrosion. Tribo-corrosion involves a synergism between wear and corrosion, since the total material loss when the two processes occur simultaneously is greater than when they act alone [8]. Insufficient resistance to tribo-corrosion limit the application of aluminium alloys [9]. For that reason, a thin layer called “thermal barrier coatings” can be formed on the surface subjected to high temperature for long time, to protect it from thermal damage. These thermal barrier coatings, usually consisting of ceramics, will protect the surface and reduce heat loss from inside to outside due to its lower thermal conductivity.

Many technologies were used to form a protective layers/coating on aluminium alloys to enhance the tribo-corrosion resistance properties of the alloy, such as laser cladding, traditional welding processes, hard anodization, plasma electrolytic oxidation and plasma-spray ceramic coatings etc. [10].

Plasma-spray ceramic (PSC) coating is considered a famous and cheap technique for cladding many metallic surfaces. It can be used to deposit metals, ceramics or even plastics on the surface of most of the metallic surfaces. Also, the thickness of the coating varies from a few micrometres to several millimetres [11–12]. Plasma Spray Ceramic Coating is a coating produced by process in which molten or softened particles are applied by impact onto a substrate [13, 14]. It was first addressed by Schoop when he studied the production of metallic particles from a molten metal to

be used as a coating at the beginning of the last century [15]. There are three main stages to form this coating. Firstly, plasma particles are created as small droplets stream [16]. Secondly, these particles are subjected to high temperature using heat source generating thermal energy. The particles' compositions get changed due to the chemical reaction between the droplet material and the flame [17]. After that, they are flattened then striking a cold surface at high velocities generating kinetic energy. A common feature of lamellar grain structure will be formed as a result of the rapid solidification and cooling processes. The general behaviours of PSC coating are considered to be porous lamellar structures [18] composed of splats with columnar grain structures and have voids and pores areas.

Among many ceramics, Al_2O_3 are the most widely used for cladding the aluminum alloys through plasma spraying. Besides its low density, high hardness & wear resistance, low cost and its wide range of available grades, it has excellent thermal stability. The Al_2O_3 coating can protect its substrate form severe and harsh environment when wear and corrosion are presented [19]. Beauvais et al., [20] studied the microstructure of plasma sprayed coating using different ceramic powders (Al_2O_3–TiO_2, Al_2O_3, ZrO_2–Y_2O_3 (YSZ) and Cr_2O_3) on 316 stainless substrates. It was found that the PSC microstructure was homogenous with low porosity. Also, micro-cracks in the Al_2O_3 coating were detected as a result of the thermal stresses developed during the process [20]. Song et al., [21] deposited Al_2O_3 and TiO_2 powders using plasma spraying method with different powers on 6063 aluminium alloy substrate. The coating has high porosity at low power source, since the parts of the particles did not completely melt and were embedded in the melted lamellar structure. As the power source increased, the un-melted particles decreased, and lamellar structure was formed with less particle sizes. Abdel-Salam et al., [22] improved the corrosion resistance of the 2014 Al alloy through hard anodizing in sulphuric acid electrolyte. They found that the addition of sulphonate significantly improve the corrosion resistance. Tabakoff and Shanov [23] studied the erosion behaviour of the plasma ceramic coating that used in compressors and turbines at high temperature. They reported that TiC coating shows better erosion resistance when exposed to fly ash and chromite particles. Wang et. al. [24] sealed the plasma sprayed alumina coating through aluminum phosphate. The results showed that the phosphate penetrates through the interface between the alumina coating and the substrate and improves the sliding wear resistance.

Most of the previous works [19-26] were focused on the wear or corrosion behaviors of plasma ceramic coating. In this research work, we planned to characterize both erosion and corrosion of

the plasma ceramic coating layer that deposited on Al 6082 alloy. The microstructure of the coating layer was investigated in detail. The hardness, erosion resistance, and corrosion behavior of the coating layer was evaluated in detail at ambient and high temperatures.

2. Experimental work

The substrate used for PSC coating was 6082-T6 aluminum alloy. The substrate specimens' discs were cut with a diameter of 25.40 mm and a thickness of 10 mm ± 0.01 mm to be fitted in the holder for erosion and electrochemistry experiments suitable for the rig available in the lab. The samples were coated using a conventional 100 kW atmospheric plasma spraying system. The powder of grey alumina contains 2.5% of titanium dioxide was feed at constant rate of 15 gm/min, using a turntable type volumetric powder feeder. The feeding and spraying distances were 24 mm and 300 mm, respectively. The microstructures of the PSC coating were investigated using scanning electron microscope equipped with EDX analyzer. The database (ICDD, International Centre for Diffraction Data) entries used were 00-046-1212 and 01-074-4629 for alpha and gamma respectively. The area of the peaks was determined using the software XPert Highscore Plus. The PSC coated layer were analyzed by X-ray diffractometer (XRD). Surface roughness of the coated surface was measured using Veeco-Wyko NT 3300S Interferometer. An Inductive Coupled Plasma (ICP) test was performed to assess the amount of ions (Al^{3+}) released from the 3.5%NaCl solution after 24 hours (for temperatures of 20°C and 80°C) of immersing the samples into the solution at different test conditions. Then, the samples were polarized up to 400 mV against the reference electrode for another 24 hours. This polarization test was theoretically compared with Faraday's Law of electropolsity that gives an indication of corrosion process of these coatings on the basis of ion movements across the coating layers. The erosion tests were performed using sand particles through Recirculation Jet Impinging Rig. These sand particles have round shape and sharp edges with an average diameter between 200 µm and 250 µm as shown in the SEM image in Figure 1. Two sand loadings (200 mg/l & 1000mg/l) and two temperatures (20°C & 70°C) were selected as the main experimental variables to go gradually from medium to highly severe erosion conditions. After erosion experiments, the weight loss measurements were recorded after 2, 5, 8 and 10 hours followed by profilometry and microscopic analysis on the surfaces of the coated samples to analyze the surface of the coated samples after erosion experiments using "Form Talysurf 120L" equipment in order to measure the surface shape, texture, profile of volumetric damage and to identify the depth of the attack and the zones which suffer the greatest degradation.

The microhardness of the coated layer and the substrate were measured (before and after the erosion test) using Knoop indenter. The shape of this type of indenter is an elongated diamond pyramid and it is more sensitive to surface conditions than Vickers test which is more suitable for the thin coatings [27].

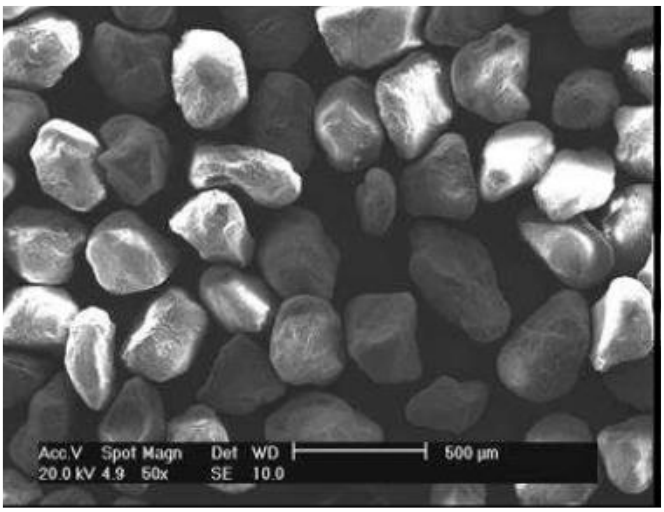

Figure 1. SEM image of sand particles used for erosion test.

3. Results and Discussions

3.1 Macro/microstructure analysis

The coated plasma spray ceramic (PSC) consisted of three different layers of about 350 µm thick, starting with a loose layer in the interface region of 87 µm as shown in Figure 2 (a). This layer is followed by the intermediate layer of approximately 250 µm and finally the top porous layer of 55 µm. The intermediate layer contains many laminar structures with white colours which could be the aluminium alloy 6082-T6. Similarly, the SEM cross-sectional image of PSC sample, shown in Figure 2 (b), reveals that the average coating thickness is about 275 – 280 µm. The dark layer (gap) at the interface is probably due to debonding of the PSC coating from the substrate. Although it is due to metallographic preparation (sectioning / polishing), it also indicates a poorer bond with the substrate.

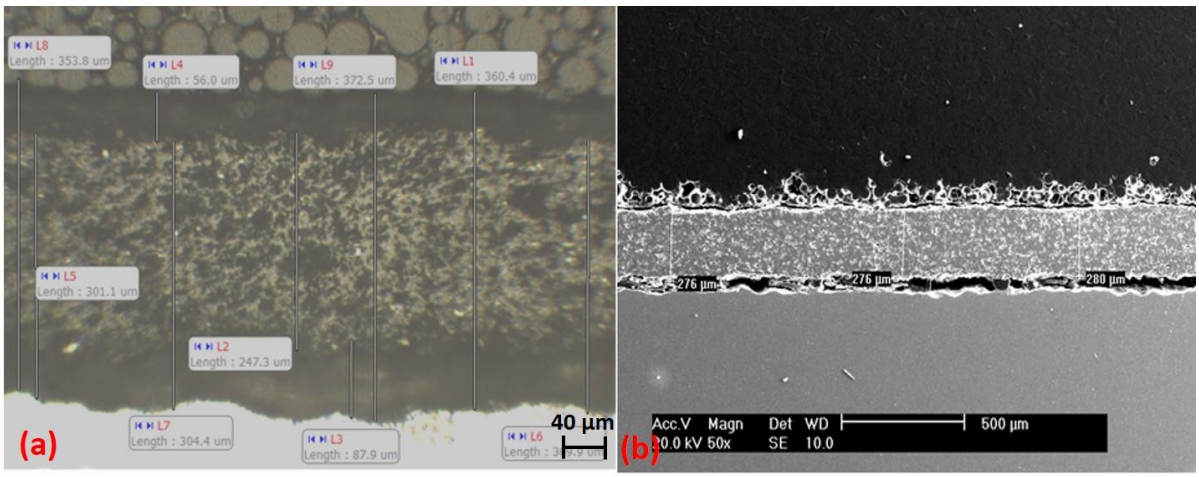

Figure 2. Cross-sectional view of PSC coating.

Microscopically, the microstructure of the plasma spray ceramic coating (Figure 3) exhibits a lamellar structure and has many porous regions. The EDX analysis (Figure 4) detected the elements of aluminium, oxygen and titanium. The PSC coating was prepared using grey alumina powder which contains 2.5% of titanium dioxide according to the supplier. According to XRD spectra shown in Figure 5, PSC coating has α-Al_2O_3 and γ-Al_2O_3 phases but with lower intensity peaks. The relative proportions of alpha alumina (α-Al_2O_3) and gamma alumina (γ-Al_2O_3) phases can be estimated from the intensity (area) of the peaks in the XRD plots for the material. Conventionally, this is achieved using the most intense peaks for each phase and using an RIR (Reference Intensity Ratio) for each phase. RIR values are normalised against corundum (alpha alumina, which has a value of 1.0). Due to peak overlap and strong scattering from the substrate, it was not possible to use the most intense peaks. Therefore, to gauge the relative proportions, less intense, but unobstructed peaks were used at 25.578° for and 19.318° for gamma. The area of the peaks was then divided by the product of the RIR and the relative intensity of the peak (from the database). The amount of alumina phases (α-Al_2O_3) available in PSC coating was 14% and Gamma alumina (γ-Al_2O_3) was 86%.

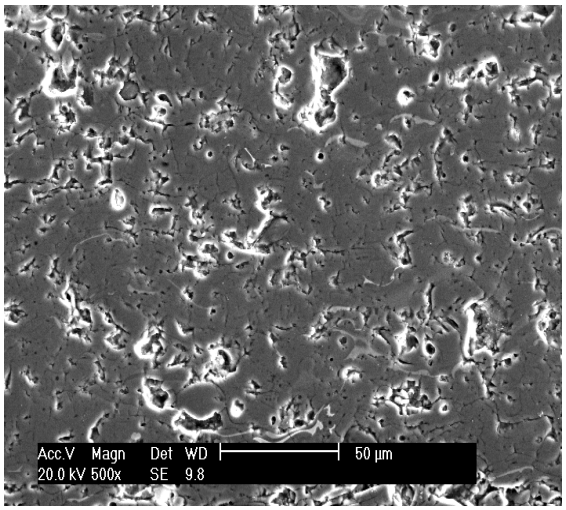

Figure 3. Microstructure of PSC.

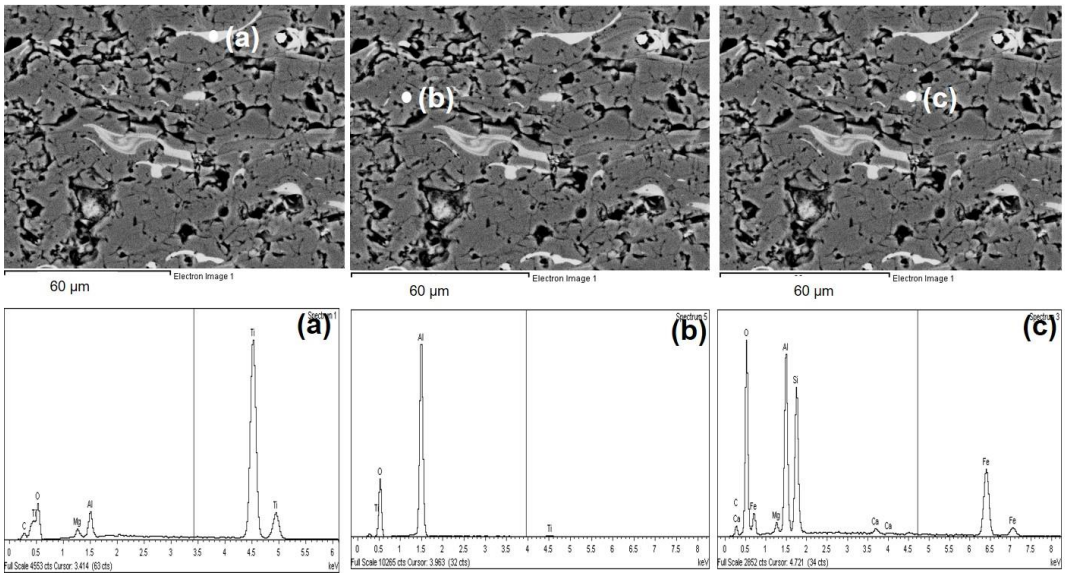

Figure 4. Detection of elements of PSC using EDX analysis.

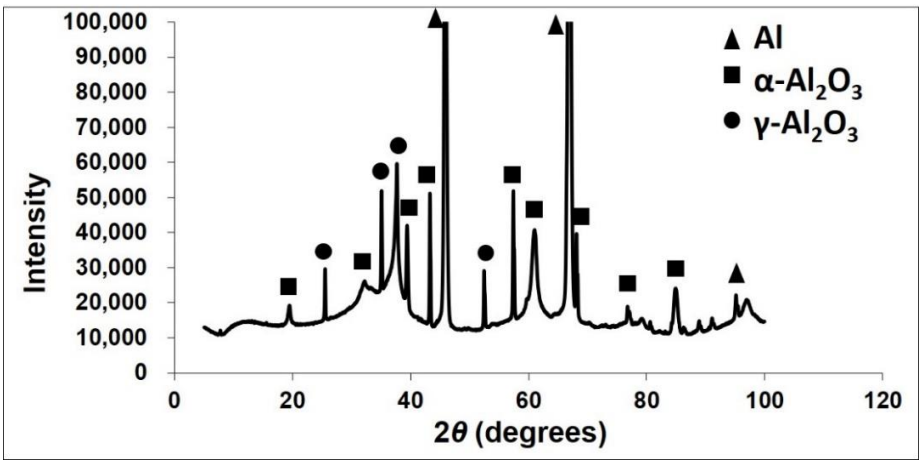

Figure 5. XRD for PSC sample; (a) full plot and (b) Zoomed scale.

3. 2. Electrochemistry

3.2.1 Inductive Coupled Plasma (ICP) Test Results

Figure 6 show the potential current versus time plots to calculate charge transfer at 400 mV for PSC sample. There was no stability of the current in the PSC sample as many variations of the curve occurs during the 24 hours polarization test and the currents were relatively high. The first increase of the current occurs at about 1000 seconds from 1.5 x 10^{-2} A/cm^2 to 3.0 x 10^{-2} A/cm^2 which could be attributed to high movements of Al^{3+} movement through the coating due to its high porosity. The current fluctuation on the polarisation curves could be attributed for electrochemistry activities taking place on the surfaces such as localised pitting corrosion in the substrate/coating interface region [28]. However, the current increases also from about 2.5 x 10^{-2} A/cm^2 to 5.0 x 10^{-2} A/cm^2 around 7000 seconds where it is expected that the PSC coating has completely removed from the substrate as shown in Figure 7. This is due to the low adhesion between the substrate and the coating where ions penetrate between them.

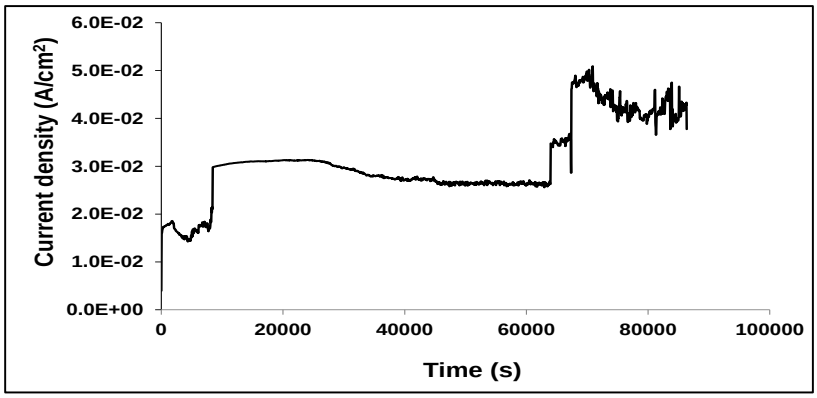

Figure 6. Current density versus time plots to calculate charge transfer for PSC at +400 mV (Ag/AgCl).

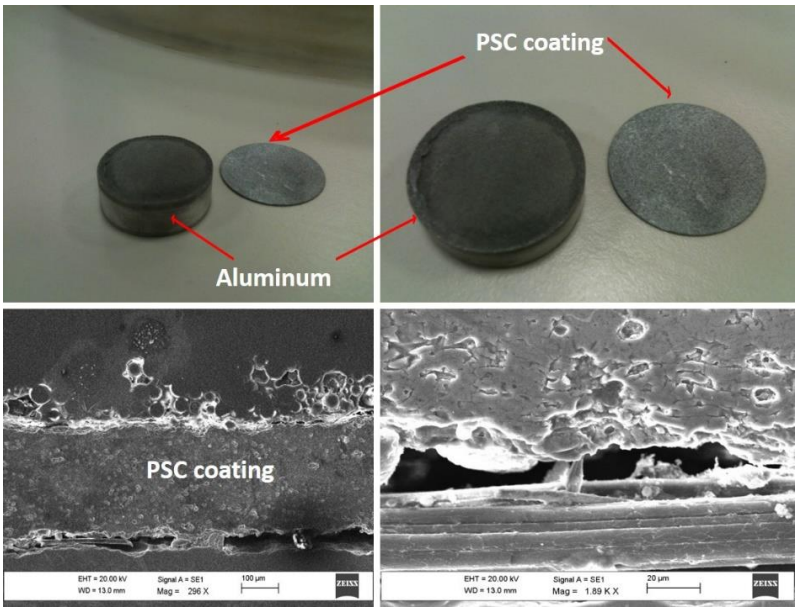

Figure 7. PSC sample after 24 hours ICP polarization Test.

3.2.2 Anodic Polarization (AP) Measurements

Figure 8 shows the results of the anodic polarization resistance for PSC sample together with Al substrate. The breakdown voltages for all materials can be determined from the anodic polarization curves at the potential value where the current increased rapidly and deviated from the initial growing rate. The values of the breakdown potentials of the materials were determined from the Excel plots and the red lines in these graphs are just to show the method and not indicating the exact E_b values. The breakdown potential (E_b) is the potential where the passive film of the surface breaks down. E_b for the ceramic materials indicate the penetration of the electrolyte ions through the coating defects to the substrate metal. It is expected that the coating would decrease the possibility of breaking down the aluminium passive film and consequently decrease the current density and improve the corrosion resistance [29-30].

The corrosion current densities for the materials were determined from the logarithmic scale of the current density in the anodic polarization curves as shown in Figure 9. The potential was shifted from the OCP value of the material to 250 mV in the opposite direction to ensure that the cathodic and anodic currents are different to measure the corrosion current density on the sample by extrapolating the anodic branch with the line from OCP value. Table 1 summarises the main

corrosion parameters of the materials that were determined from the DC electrochemistry plots (anodic polarisation curves). Therefore, PSC coating has lower corrosion current density (2.6E-07 A/cm^2) under static anodic polarization tests.

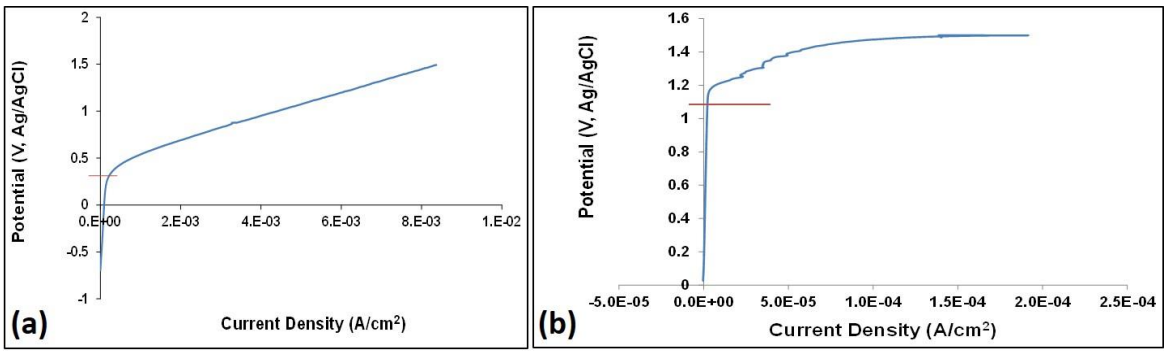

Figure 8. AP Measurements for (a) aluminium substrate and (b) PSC coating.

Table 1. Summary of corrosion parameters of the materials.

Corrosion Parameter	**PSC**	**Al**
Open circuit potential *(*OCP*)* [V]	-0.76	-0.7
Breaking down potential (E_b) [V]	1.12	0.2
Corrosion current density (i_{corr}) [A/cm^2] from AP Curve	2.6E-07	1.2E-05

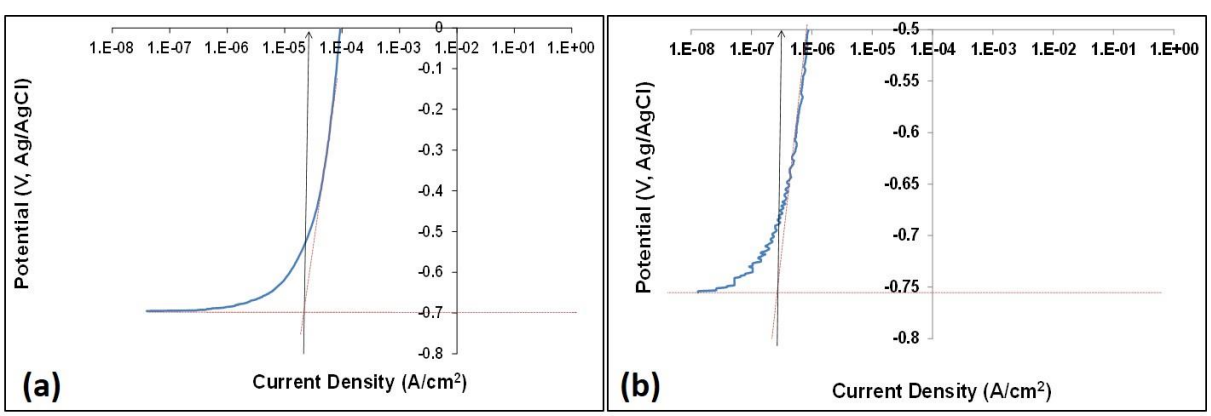

Figure 9. Determination of corrosion current density for (a) Al substrate and (b) PSC.

3.2.3 AC Impedance Plots for Plasma Spray Ceramic (PSC) Surface

The arc radius in the Nyquist plot of PSC coating was slightly increased after the full period of immersion test (Figure 10 (a)). This corresponds to the minimal change in the total resistance from the Bode plot shown in Figure 10 (b). The aluminium substrate can be seen after the corrosion test which indicates that relatively high amount of PSC coating degradation has occurred due to this chemical reaction.

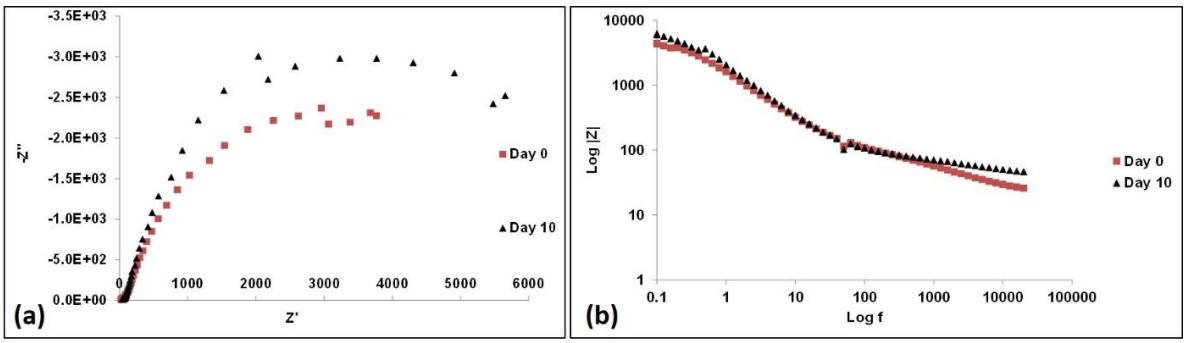

Figure 10. (a): Nyquist plots and (b): Bode plots for PSC at different immersion times.

The AC impedance data was fitted using the circuit model (Figure 11) and the results are shown in Figure 12 for Day 10 of the immersion period. Although there is no significant change in the arc radius of the Nyquist plot of PSC after the full period of immersion test, the total resistance was fluctuating between these two end points as shown in Figure 13. The increase of the resistance between day 2 and day 5 corresponds to the formation of the corrosion products at the coating/substrate interface that initiated due to ions transfer in the pores regions of PSC surface. The resistance and phase constant element were fluctuating during the period of the test (Figure 13) which indicate that part of the PSC coating was delaminated [31].

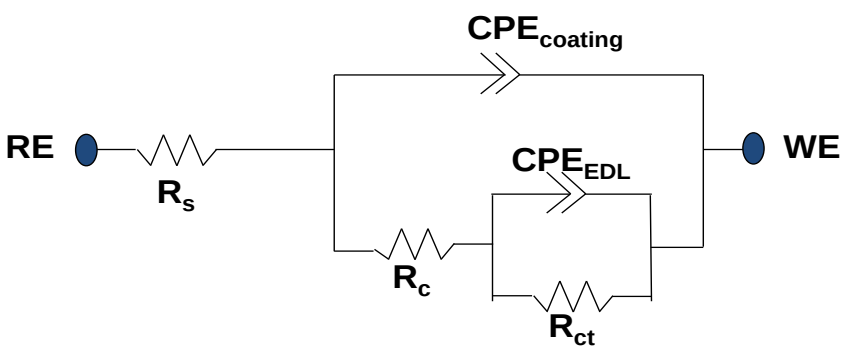

Figure 11. Modified circuit model for PSC coating.

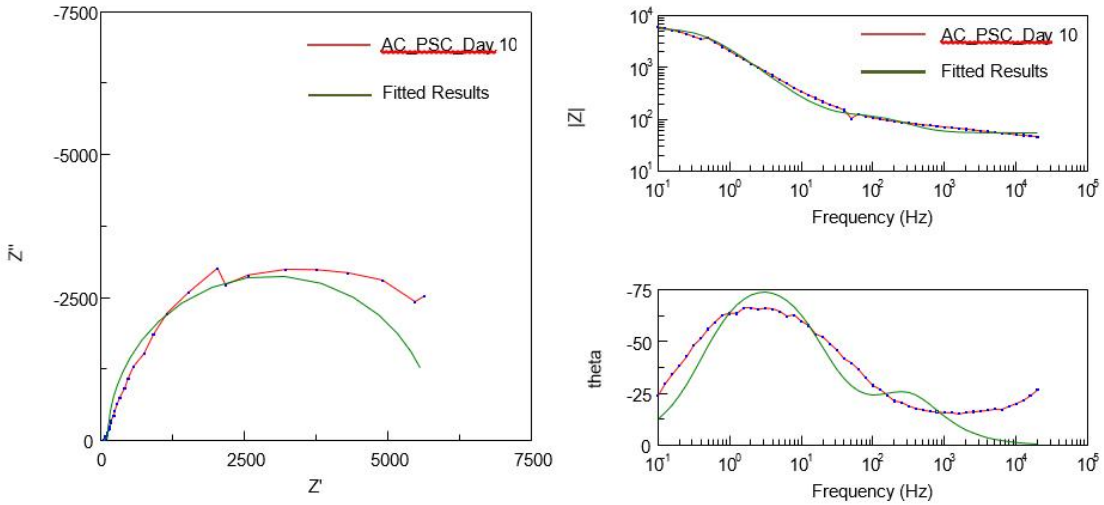

Figure 12. Fitted data for PSC coating at day 10.

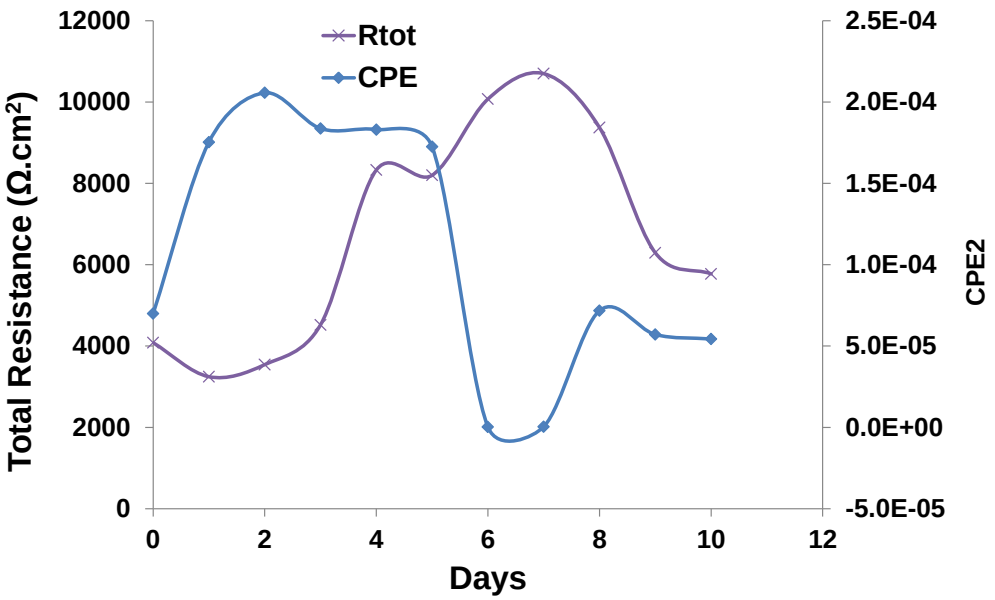

Figure 13. Time dependence of the R_{tot} and CPE_2 for PSC coating after different exposure times.

3.4. Erosion Test Results

This part presents the results of erosion experiments performed on the samples of the aluminium substrate and the PSC coatings. Figure 14 shows the weight loss measurements of the materials for ten hours experiments under low (200 mg/l) and high (1000 mg/l) sand loadings at temperatures

of 20 and 70 ºC. The weight loss measurements were recorded after 2 hours, 5 hours, 8 hours and 10 hours to observe how the wear rate of the materials changes with time. The data points have been fitted with either linear regression line or polynomial curve according to the weight loss trend for each material. A consistent increase in the wear losses has been observed with increasing both time and sand loading as expected. Generally, the PSC coating exhibits poor erosion resistance in the test conditions when compared to aluminium substrate at both sand loading 200 mg/l and 1000 mg/l. The PSC coating has high erosion rate and its weight loss is more than the aluminium substrate after five hours at low sand loading and four hours at high sand loading. Moreover, the erosion rates observed in elevated temperature tests are higher than in room temperature tests for the PSC coated samples and aluminium substrate.

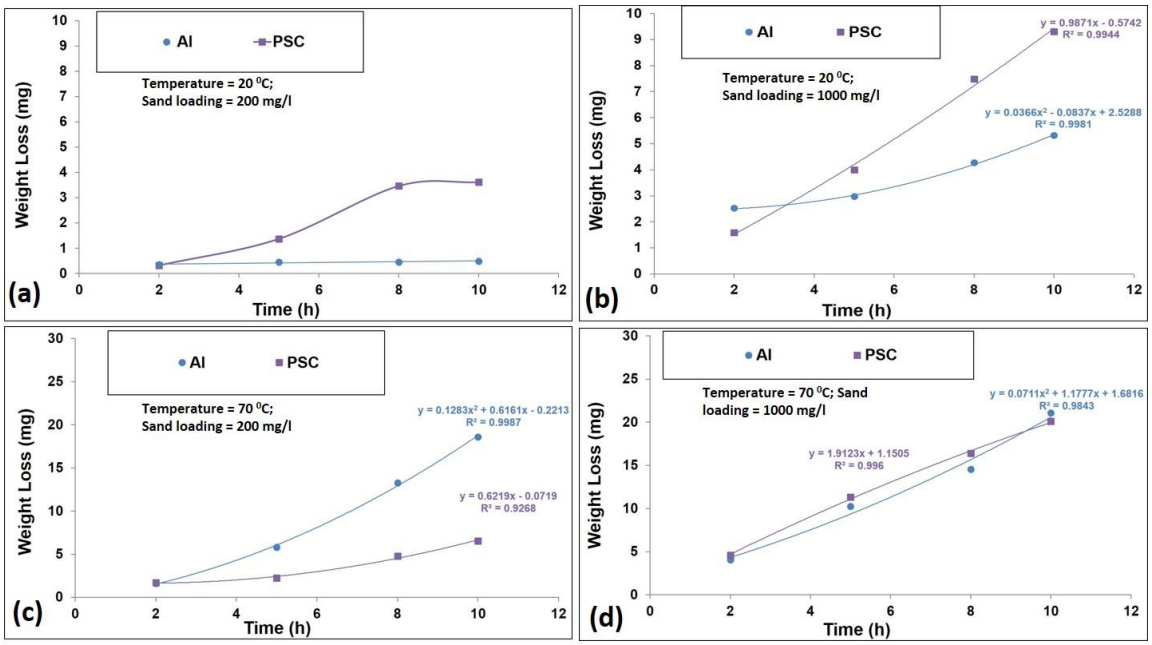

Figure 14. Weight loss measurements at different conditions after 10 hours.

It has been observed that the aluminium substrate has good erosion resistance and has a linear wear rate at low sand loading and low temperature. When the sand lading was increased to 1000mg/l, large amount of material loss was observed, which match the results of Zhang et al., [32] and Costa et. Al. [33]. It is noticed that a large amount of PSC material has been removed due to the impact loading. Also, its wear loss rate increases sharply compared to aluminium sample where the erosion rate increases gradually. This indicates that the removed materials of PSC take place as cracks on the surface followed by chipping off the coating since its surface exhibits brittle material

fracture. This could be attributed to the low adhesion bonding and pores as shown between the PSC coating and the substrate in Figure 15.

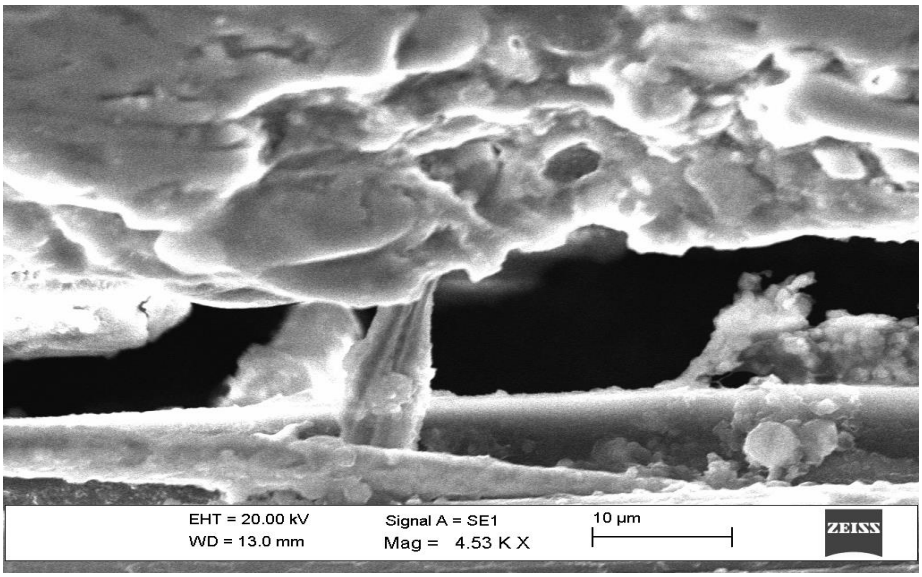

Figure 15. High gap size between PSC coating and Al substrate.

3.5. Hardness measurements

The hardness values of the tested materials were obtained before performing the erosion tests to study the effect on the wear response and the results shown in Figure 16. Before the erosion test, the micro-hardness values for the coating layer are much harder than the Al substrate. The coating layer hardness increases as the distance from the substrate increases until near the middle of the coating (100 μm). After that, the hardness decreases as the distance approaches the resin side of the coating. Also, the hardness measurements of the eroded regions of the coatings were compared with the un-eroded surfaces after the test and it is obvious that the hardness for the eroded surface is higher for all materials. The increase of the material's hardness after the erosion tests is expected since there is a work hardening undergoing on the surface due to the effect of the impact particles loading.

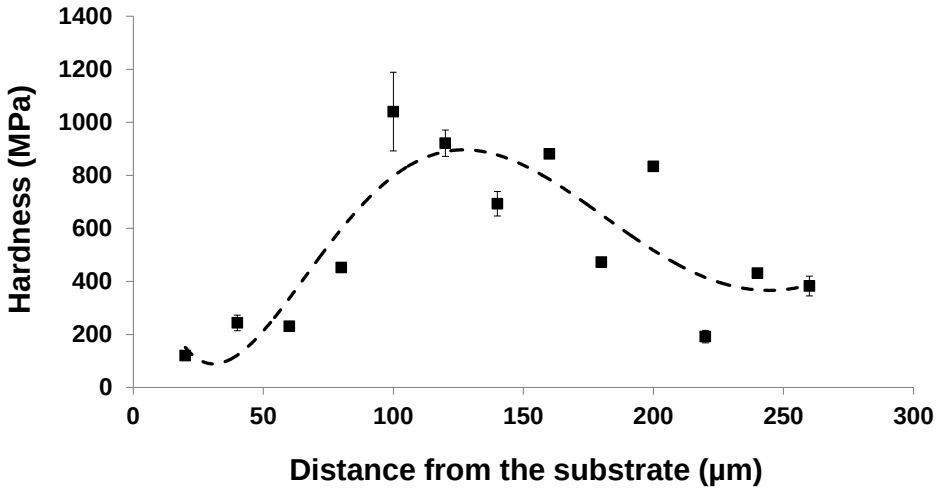

Figure 16: Distribution of hardness values across PSC coating (Knoop Test, Load = 25 g).

3.6. Talysurf Tests

Figure 17 shows the surface textures of the tested samples after ten hours tests for different sand loadings (200 and 1000 mg/l) and different temperatures (20 ©C and 70 ©C). The 3-D profile of the sample was captured to show the affected zone of the surface and its type in terms of the deformation type such as plastic deformation, cutting chip, etc. As clearly shown in Figure 17 (b) and (d), the sand lading had a greater effect on the erosion rate more than the temperature. Also, the materials' volume loss due to impact particles were calculated to be compared with the weight loss measurements.

Regarding the coating density, it has been approximately determined by coating porosity which can be studied from optical or SEM images. Limited studies have measured the coating density. For example, Curran and Clyne [34] has suggested that the PEO density is summation of phase densities in the coating (α-Al_2O_3, γ-Al_2O_3 and amorphous alumina) which theoretically equals to 3.69±0.25 g/cm^3. However, this will depend on the phases available in the coating and also affected by the thickness of the coating.

The density of the removed materials after erosion can be calculated by dividing the measured weight loss over the volume loss data as shown in Figure 18. There are two reasons that can explain the anomalous densities of the removed materials against their theoretical values (2.7 g/cm^3 for the aluminium substrate and approximately 3.69±0.25 g/cm^2 for the coatings). Firstly, it should be

noted the removed materials sometimes consists of the coating part and the substrate which have different densities. Secondly, the porosity has main effect of the density of the material as the pore space in the eroded material will increase due to the impact of solid particles [35]. As a result, the volume of the material will decrease and consequently increase its density as shown in Figure 18. Thirdly, it is assumed that the measured volume loss from the Talysurf analysis is less than the actual volume loss of the material. The volume of the removed top layer could not be determined using this technique. Therefore, most of the measured densities of the materials under different test conditions are higher than their actual density values.

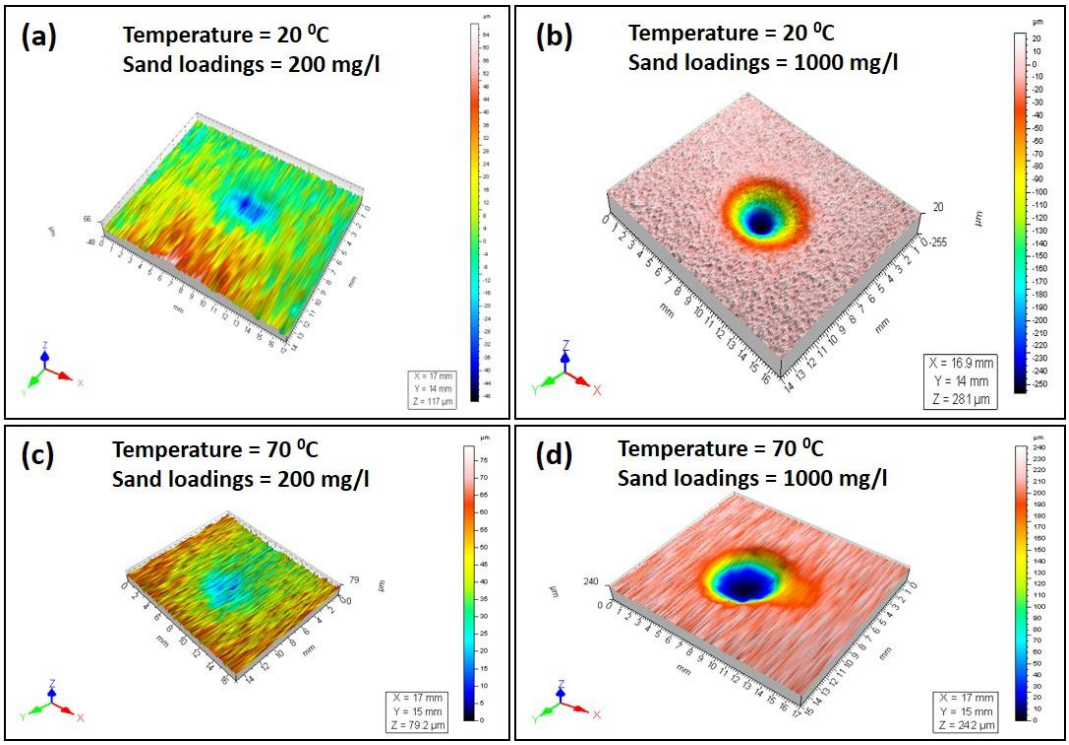

Figure 17. 3-D Profilometry tests for PSC coating after erosion test of 10 hours.

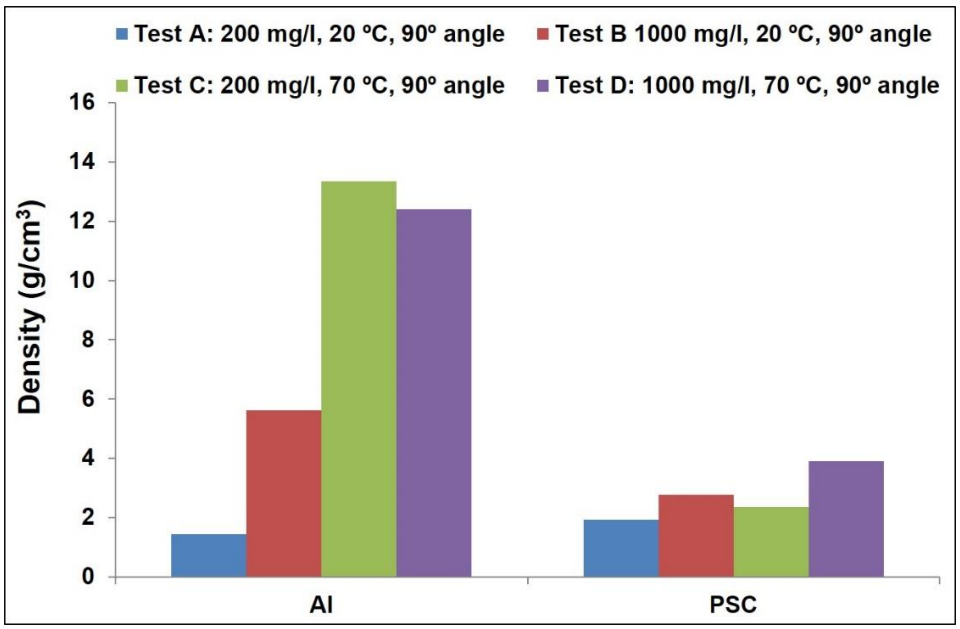

Figure 18. Density of the removed materials after 10 hours erosion tests.

4. Conclusions

In this work, aluminum 6082-T6 was cladded with the plasma sprayed Al_2O_3 coating process. The macro/microstructures of the coated specimens were investigated using optical and scanning electron microscopes. An inductively coupled plasma test was performed after immersion in 3.5% NaCl solution for 24 hours (for temperatures of 20°C and 80°C). The erosion tests were performed with water carrying sand particles at different sand loadings (200mg/l and 1000mg/l) and two temperatures (20°C and 70°C). After erosion experiments, the weight loss measurements were recorded followed by profilometry and microscopic analysis. The micro-hardness of the coated layer and the substrate were measured. The results of this study led to the following conclusions:

- The coated layer consisted of three different layers of about 350 µm thick, starting with a loose layer in the interface region followed by laminar intermediate layer and finally top porous layer. The hard-anodizing coating has a higher roughness value compared with the Al substrate.
- The coated layer was consisted of approximately 86% Gamma alumina (γ-Al_2O_3) and 14% alumina phases (α-Al_2O_3).
- There was no stability of the current in the coating during the polarization test. The coating shows lower corrosion current density under static anodic polarization tests.

- During the erosion test, a consistent increase in the wear losses has been observed with increasing both time and sand loading.
- Compared to the aluminium substrate, the PSC coating exhibits poor erosion resistance at low temperature, while the erosion rates observed for the PSC coating in elevated temperature are much lower than aluminium substrate.
- The coating showed higher hardness values compared to aluminum substrate.

5. References

[1] H. Mraied, W. Cai, and A. A. Sagüés, "Corrosion resistance of Al and Al–Mn thin films," Thin Solid Film. Vol. 615, pp. 391-401, 2016. doi.org/10.1016/j.tsf.2016.07.057.

[2] R.W. Revie, and H.H. Uhlig, "Corrosion and Corrosion Control: An Introduction to Corrosion Science and Engineering, fourth edition, Wiley-Interscience, 2008, [Online]. Available: http://onlinelibrary.wiley.com/book/10.1002/9780470277270. [Accessed: July. 15, 2018].

[3] A.W. Momber, T. Marquardt, "Protective coatings for offshore wind energy devices (OWEAs)," J. Coat. Technol. Res. Vol. 15, pp. 13–40, 2018. https://doi.org/10.1007/s11998-017-9979-5.

[4] A. López, R. Bayón, F. Pagano, A. Igartua, A. Arredondo, J.L. Arana, and J.J. González, "Tribocorrosion behaviour of mooring high strength low alloy steels in synthetic seawater," Wear Vol. 338-339, pp. 1-10, 2015. https://doi.org/10.1016/j.wear.2015.05.004.

[5] G. A. El-Mahdy, and K.B. Kim, "AC impedance study on the atmospheric corrosion of aluminium under periodic wet-dry conditions," Electrochim. Acta. Vol. 49(12), pp. 1937-1948, 2004. doi:10.1016/j.electacta.2003.12.022

[6] M. Navaser, and M. Atapour, "Effect of Friction Stir Processing on Pitting Corrosion and Intergranular Attack of 7075 Aluminum Alloy.," J. Mater. Sci. Technol. Vol. 33 (2), pp. 155-165, 2017. doi: 10.1016/j.jmst.2016.07.008

[7] M. de Bonfils-Lahovary, L. Laffont, and C. Blanc, "Characterization of intergranular corrosion defects in a 2024 T351 aluminium alloy." Corros. Sci. vol.119, pp. 60-67, 2017. doi:10.1016/j.corsci.2017.02.020

[8] C.N. Panagopoulos, and E.P. Georgiou, "Corrosion and wear of 6082 aluminium alloy," Tribol. Int. vol. 42(6), pp. 886-889, 2009. doi.org/10.1016/j.triboint.2008.12.002

[9] A. López-Ortega, R. Bayón, J.L. Arana, A. Arredondo and A. Igartua, "Influence of temperature on the corrosion and tribocorrosion behaviour of high-strength low alloy steels used in offshore applications," Tribol. Int. vol. 121, pp. 341–352, 2018. https://doi.org/10.1016/j.triboint.2018.01.049.

[10] H. Li, Z. Ke, J. Li, L. Xue, and Y. Yan, "An effective low-temperature strategy for sealing plasma sprayed Al2O3-based coatings," Journal of the European Ceramic Society 38, pp.1871–1877, 2018. http://dx.doi.org/10.1016/j.jeurceramsoc.2017.09.051

[11] P. Wang and J. P. Li, "The formation mechanism of the composited ceramic coating with thermal protection feature on an Al-12Si piston alloy via a modified PEO process," J. Alloys Compd. Vol. 682, pp. 357–365, 2016.

[12] J. Yamabe, S. Matsuoka and Y. Murakami, "Surface coating with a high resistance to hydrogen entry under high-pressure hydrogen-gas environment," Int. J. Hydrogen Energy vol. 38, pp. 10141–10154, 2013.

[13] R. Kromer, S. Costil, C. Verdy, S. Gojon, and H. Liao, "Laser surface texturing to enhance adhesion bond strength of spray coatings – Cold spraying, wire-arc spraying, and atmospheric plasma spraying," Surf. Coat. Technol. Vol. 352, pp. 642–653, 2018. doi.org/10.1016/j.surfcoat.2017.05.007

[14] K. Yang, J. Rong, C.G. Liu, H.Y. Zhao, S.Y. Tao and C.X. Ding, "Study on erosion–wear behavior and mechanism of plasma-sprayed alumina-based coatings by a novel slurry injection method," Tribo. Int. vol. 93, pp.29–35, 2016.

[15] H. Singh, and B. S. Sidhu, "Use of plasma spray technology for deposition of high temperature oxidation/corrosion resistant coatings-a review," Mater. Corros. VOL. 58(2), PP. 92-102, 2007. DOI: 10.1002/maco.200603985

[16] S. Kumar, A. Kumar, D. Kumar, and L. Jain, "Thermally sprayed alumina and ceria-doped-alumina coatings on AZ91 Mg alloy," Surf. Coat. Tech. vol. 332, pp. 533-541, 2007. doi:10.1016/j.surfcoat.2017.05.09

[17] D. Thirumalaikumarasamy, K. Shanmugam, and V. Balasubramanian, "Corrosion performances of atmospheric plasma sprayed alumina coatings on AZ31B magnesium alloy under immersion environment," J. Asian Ceram. Soc. vol. 2(4), pp. 403-415, 2014. doi.org/10.1016/j.jascer.2014.08.006

[18] T. Q. Nakamura, G. Berndt, and C. Christopher "Effects of Pores on Mechanical Properties of Plasma-Sprayed Ceramic Coatings," Journal of the American Ceramic Society, vol 83(3), pp. 578-584, 2000.

[19] S.H. Yao, "Comparative study on wear performance of traditional and nanostructured Al2O3-13 wt.% TiO2 air plasma spray coatings," Ceramics- Silikáty vol. 59, pp. 59–63, 2015.

[20] S. Beauvais, and V. Guipont, "Process-microstructure-property relationships in controlled atmosphere plasma spraying of ceramics," Surf. Coat. Technol., vol. 183(2-3), pp. 204-11, 2004.

[21] R. G. Song, and C. Wang,"Microstructure and properties of Al2O3/TiO2 nanostructured ceramic composite coatings prepared by plasma spraying," J. Alloys Compound., vol. 544(0), pp. 13-18, 2012.

[22] O. E.Abdel-Salam, M. A. Shoeib, and H. Ashour Elkilany, "Characterization of the hard anodizing layers formed on 2014-T3 Al alloy, in sulphuric acid electrolyte containing sodium lignin sulphonate," Egyptian Journal of Petroleum, Article in Press, https://doi.org/10.1016/j.ejpe.2017.07.014

[23] W. Tabakoff, and V. Shanov. "Erosion rate testing at high temp. for turbo machinery use." Surf. Coat. Technol. Vol. 76 – 77, Part I, pp. 75 –80, 1995.

[24] Q. Wang, C. S. Ramachandran, G. M. Smith, S. Sampath, "Sliding wear behavior of air plasma sprayed Al2O3 coatings sealed with aluminum phosphate," Tribo. Int., vol. 116, pp. 431–439, 2017. http://dx.doi.org/10.1016/j.triboint.2017.08.002

[25] M. Daroonparvar, M. Yajid, N. Yusof, and H. Rad, "Fabrication and properties of triplex NiCrAlY/nano Al2O313%TiO2/nano TiO2 coatings on a magnesium alloy by atmospheric plasma spraying method," J. Alloys Compd. Vo. 645, pp. 450–466, 2015.

[26] E. Colonetti, E. Kammer, and A. Junior, "Chemically-bonded phosphate ceramics obtained from aluminum anodizing waste for use as coatings," Ceram. Int. vol. 40, pp. 14431–14438, 2014.

[27] C. Sujaya, H. Shashikala, G. Umesh and A. C. Hegde, (2012). "Hardness and electrochemical behaviour of ceramic coatings on Inconel." J. Electrochem. Sci. Eng. Vol. 2(1), pp. 19-31. 2012.

[28] M. Thammachart, "Corrosion Mechanisms of Chemically Bonded Composite Sol-Gel (CB-CSG) Al2O3 Coated Systems in Aqueous Environment," Edinburgh, Heriot-Watt University, PhD: 297, 2005.

[29] H. Lee, J. K. Singh, and M. A. Ismail, "An effective and novel pore sealing agent to enhance the corrosion resistance performance of Al coating in artificial ocean water, Sci Rep. 2017; 7: 41935. Published online 2017 Feb 3. doi: 10.1038/srep41935

[30] Y. Shi, B. Yang and P. K. Liaw, "Corrosion-Resistant High-Entropy Alloys: A Review," Metals, vol. 7, pp. 43-61, 2017. doi:10.3390/met7020043.

[31] A. A. Olajire, "Corrosion inhibition of offshore oil and gas production facilities using organic compound inhibitors - A review," J. Mol. Liq. Vol. 248, pp. 775-808, 2017. doi:10.1016/j.molliq.2017.10.097

[32] G. A. Zhang, and L. Y. Xu, "Investigation of erosion-corrosion of 3003 aluminium alloy in ethylene glycol-water solution by impingement jet system," Corrosion Science, vol. 51(2), pp. 283-290, 2009.

[33] A. Costa, and G. Macedonio, “Viscous heating in fluids with temperature-dependent viscosity: implications form agma flows,” Nonlinear Processes in Geophysics, vol. (20), pp. 101-111, 2003.

[34] J.A. Curran, and T.W. Clyne, “Thermo-physical properties of plasma electrolytic oxide coatings on aluminium,” Surf. Coat. Technol. Vol.199(2-3), pp. 168-176, 2005. doi:10.1016/j.surfcoat.2004.09.037.

[35] A. Nandi, and I. Lufman, "Erosion Related Changes to Physicochemical Properties of Ultisols Distributed on Calcareous Sedimentary Rocks." Journal of Sustainable Development, vol. 5(8), pp.52-68, 2012.